Int. J. Nanosci. Nanotechnol., Vol. 20, No. 2, June 2024, pp. 143-159
DOI: 10.22034/ijnn.2024.2005501.2391

Short Communication

Contemporary Advances in Metal Oxide Doped Polypyrrole Composites: A Comprehensive Review

Nandini V. Iyer[1,2], Ganesh L. Agawane[3], Chandan Patel[3], Jayant A. Kher[2] and Shekhar D. Bhame[1,*]

[1]Symbiosis Institute of Technology, Symbiosis International (Deemed University), 412115, Lavale, Pune, India
[2]Department of Applied Sciences, COEP Technological University, 411005, Pune, India
[3]Department of Chemistry, Faculty of Science and Technology, JSPM University, 412207, Pune, India

(*) Corresponding author: shekhar.bhame@sitpune.edu.in
(Received: 29 June 2023 and Accepted: 10 April 2024)

Abstract

Intrinsically conducting polymers (ICPs) have revolutionized materials science with their versatile applications in electronics, sensors, and energy storage. This review explores the synthesis, properties, and applications of polypyrrole (PPy) and its hybrid nanocomposites with metal oxides, emphasizing advancements in electrical conductivity, stability, and performance. PPy, a prominent conducting polymer, is synthesized through chemical polymerization or electrochemical methods and exhibits high conductivity and mechanical flexibility. Doping PPy with metal oxides like nickel oxide (NiO) and tungsten oxide (WO_3) enhances its properties for various applications. PPy-NiO composites show improved conductivity and dielectric properties, while PPy-WO3 composites demonstrate superior electrochemical performance in supercapacitors. This review highlights recent advancements in synthesizing and characterizing these composites, including X-Ray Diffraction (XRD), Ultraviolet-Visible Spectroscopy (UV-VIS), and Raman Spectroscopy. The findings underscore the potential of PPy-metal oxide composites in advancing technologies such as energy storage, corrosion protection, and sensor development.

Keywords: *Conducting Polymers, Polypyrrole, Metal Oxides, Doping, Electrical Properties.*

1. INTRODUCTION

About four decades ago, intrinsically conducting polymers (ICPs) were added to the list of modern materials, opening numerous applications. Important ICPs include polyacetylene, polyaniline, polypyrrole, polyfuran, polythiophene, and more. Polysulfur nitride ([SN]x), discovered by Walatka et al. [1] in 1973, was the first inorganic conducting polymer. In the late 1970s, MacDiarmid, Shirakawa, and Heeger identified the semiconductor properties of organic polyethene through chemical polymerization. Dr. Heeger's team enhanced polythiophene-based diodes, creating a notable polythiophene LED in 2003 [2].

Conducting polymers are often doped with metal particles to enhance their properties, such as stability, flexibility, capacitance, mechanical strength, thermal stability, and corrosion resistance. These doped polymers are referred to as hybrid conducting polymers [3]. Common additives include metal powders, metal oxides, graphene, and graphene oxide [4]. Chemical polymerization and electrochemical synthesis are established methods for creating conducting polymers. Chemical polymerization uses oxidizing agents like

ammonium persulfate and iron oxide, while electrochemical synthesis employs a three-electrode system for precise control over polymerization and doping [5].

ICPs are used in electrocatalysts, sensors, electrochemical devices, supercapacitors, and corrosion protection [6]. For example, polypyrrole (PPy) is commonly used in lithium-ion batteries due to its high stability and performance. PPy/aluminium oxide solar cells offer superior conversion efficiency compared to silicon-based ones. Polyaniline (PANi) and PPy are popular in supercapacitors for their low cost, stability, and high conductivity [7].

Conducting polymers are also effective in preventing corrosion. Polyaniline-epoxy coatings shield steel surfaces [8], while composites like PANi-TiO_2 and PPy/tungstate protect mild steel and aluminium, respectively [9, 10]. In energy applications, conducting polymers act as electrocatalysts and photocatalysts, improving charge transfer efficiency [11]. For instance, PPy/ TiO_2 nanocomposites have shown enhanced photocatalytic degradation of Rhodamine B [12].

ICPs are vital in gas, biosensors, optical, and chemiresistors. They detect gases, glucose, and urea due to their electron donor-acceptor properties and ease of delocalization [13]. Biomedical applications include drug delivery, tissue engineering, diabetes monitoring, and biomedical implants. Conducting polymers are used in drug delivery systems for their biocompatibility, with dopants like carbon nanotubes and TiO_2 enhancing surface area for better drug capacity [14].

This review explores the synthesis methods, characteristics, and applications of polypyrrole and its nanocomposites with metallic oxides. The oxidative chemical route is the most common synthesis method, utilizing various dopants. Electrochemical techniques are also employed to synthesize doped PPy thin films. Characterization methods include X-Ray Diffraction (XRD), Ultraviolet-Visible Spectroscopy (UV-VIS), Raman Spectroscopy, Fourier Transform Infrared Spectroscopy (FTIR), Field Emission Scanning Electron Microscopy (FESEM), Transmission Electron Microscopy (TEM), conductivity measurements, XPS, and cyclic voltammetry. The applications of PPy-metal oxide nanocomposites are examined for electrical conductivity, supercapacitance, and gas sensing.

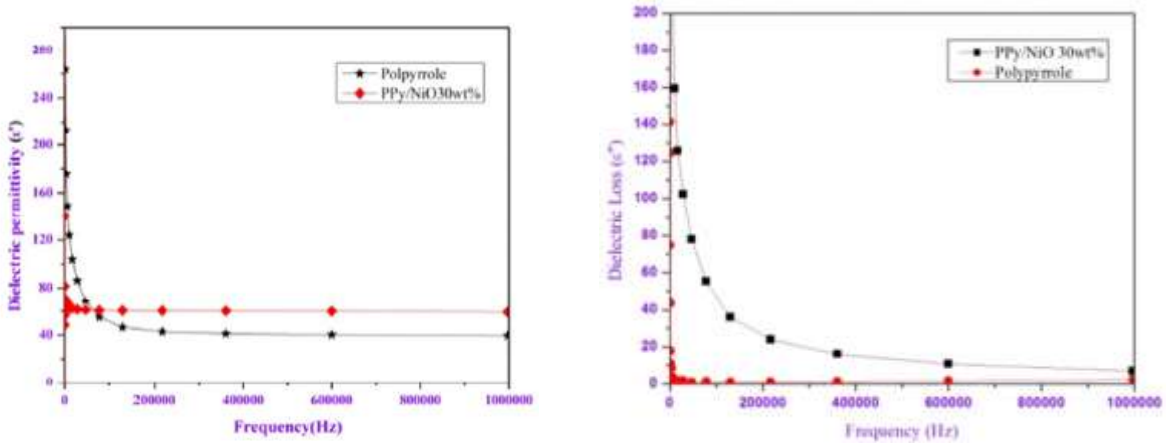

Figure 1. *(a) Dielectric permittivity Vs Frequency, (b)Dielectric Loss Vs Frequency for PPy-NiO NCs(30wt%). Reproduced from ref [23] with permission.*

2. POLYPYRROLE

Polypyrrole (PPy) is a leading conducting polymer due to its high conductivity, flexibility, ease of preparation, stability, and excellent mechanical properties [15]. It is widely applied in electronic and electrochromic devices and sensors as a stationary phase, membrane separators, capacitors, and supercapacitors [16]. Pyrrole monomer polymerizes to form

black conducting powder using oxidizing agents like iron chloride and ammonium persulfate. PPy can be synthesized in aqueous solutions and electrochemical methods, with the chemical method being more suitable for composite preparation.

PPy's conductivity, crucial in analytical applications, arises from its non-degenerate conduction band dominated by polarons and bipolarons [17]. The electrical conductivity depends on factors like electrolyte nature and concentration, counterions, doping level, current density, synthesis conditions, and solvent [18]. Conductivity can reach up to 500 S/cm under optimal polymerization conditions. The pulse potential technique in electrochemical synthesis produces smoother films with higher conductivity compared to the constant potential mode [19]. The electrolyte temperature during the synthesis affects PPy film structure, with lower temperatures leading to longer conjugation lengths, better structural networks, fewer defects, and higher conductivity. Doping enhances mechanical strength and conductivity. PPy is extensively used in sensors, membranes, and rechargeable batteries due to its electroactivity and switching properties [20]. Researchers have synthesized and characterized PPy nanocomposites with metal oxides like NiO, WO_3, ZnO, SnO_2, TiO_2, MnO_2, and Y_2O_3 for various applications.

3. COMPOSITES OF POLYPYRROLE -NICKEL OXIDE (PPy-NiO)

Nickel Oxide has a cubic crystalline structure that resembles the NaCl structure [21]. NiO has a partially filled 3d band and is supposed to be a good conductor. However, strong coulomb repulsion (a correlation effect) between the d-electrons makes NiO a wide band gap Mott-Insulator. Thus, NiO has an electronic structure that is neither simply free electron-like nor completely ionic but a mixture of both. In the NiO-doped PPy nanocomposite, NiO increases the conductivity of the pristine PPy to a certain extent according to its percentage of addition to PPy. Adding NiO in PPy leads to making useful super-capacitors, sensors, and cathode electrochromic devices [22]. The various synthetic routes, characterization techniques and applications of PPy-NiO are highlighted.

Hajeebaba K. Inamdar et al. [23,24] characterized the pure polypyrrole and the PPy/NiO (30 wt. %) nanocomposites. The dielectric properties like dielectric permittivity and dielectric loss are plotted in **Figure 1 (a, b)** in the graphs against the frequency of PPy/NiO (30 wt. %). The proposed composites exhibit a rapid decrease in the values of ε' (dielectric constant) and ε" (dielectric loss) as the frequency increases, indicating significant dielectric dispersion.

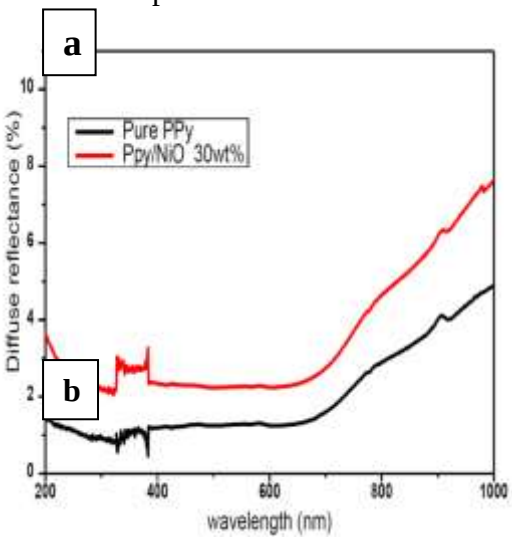

Figure 2. *DRS spectra of (a) PPy (b) PPy/NiO (30 wt%). Reproduced from ref [24] with permission.*

K. Inamdar et al. used aloe vera gel as a fuel and nickel nitrate hexahydrate ($NiNO_3)_2.6H_2O$) as a powder to produce nickel oxide nanoparticles. These nanoparticles were incorporated in the PPy matrix using the chemical polymerization method, and the PPy-NiO composites were characterized. The diffuse reflection spectra (DRS) of pure PPy and 30 wt % NiO-doped PPy (**Figure 2**) indicate that the bandgap at 1.84 eV is primarily caused by the matrix's arrangement and mess as well as the

bandgap's transformation of the energy distribution.

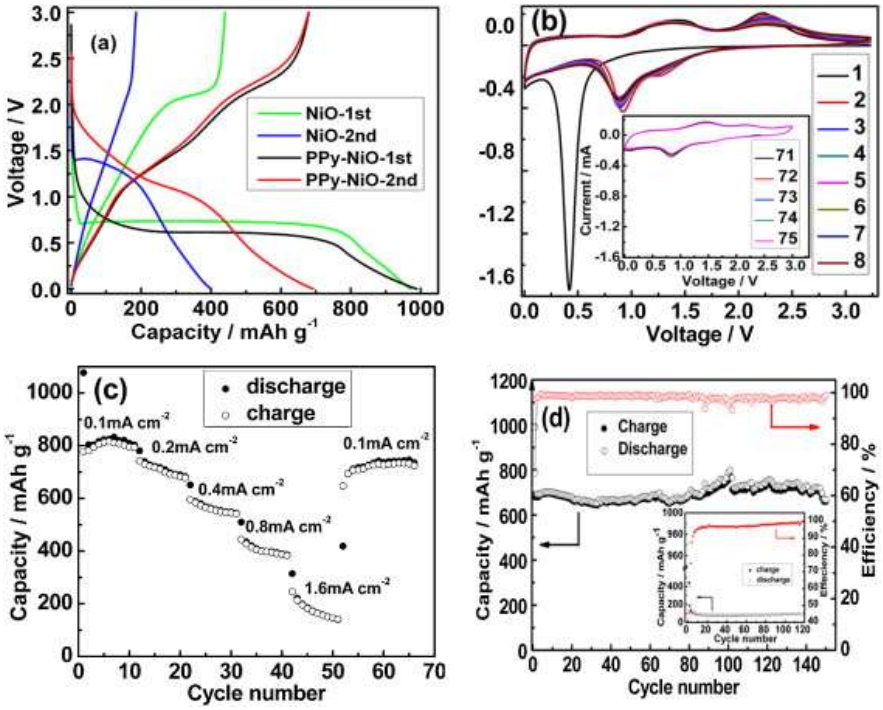

Figure 3. *The electrochemical performances of the PPy–NiO composite between 0.0 and 3.0 V vs. Li^+/Li. (a) comparison of the potential profiles of the PPy–NiO composite and commercial NiO in the first two cycles; (b) the CV plots of the PPy–NiO composite in the first 8 cycles (the inset is for the CV plots from 71st to 75th cycles) at a scan rate of 0.1 mV s^{-1}; (c) the rate performance and (d) the galvanostatic (current density 0.1 mA cm^{-2}) cycling performance (the inset is for the lithium storage capacity of pure NiO). Reproduced from ref [66] with permission.*

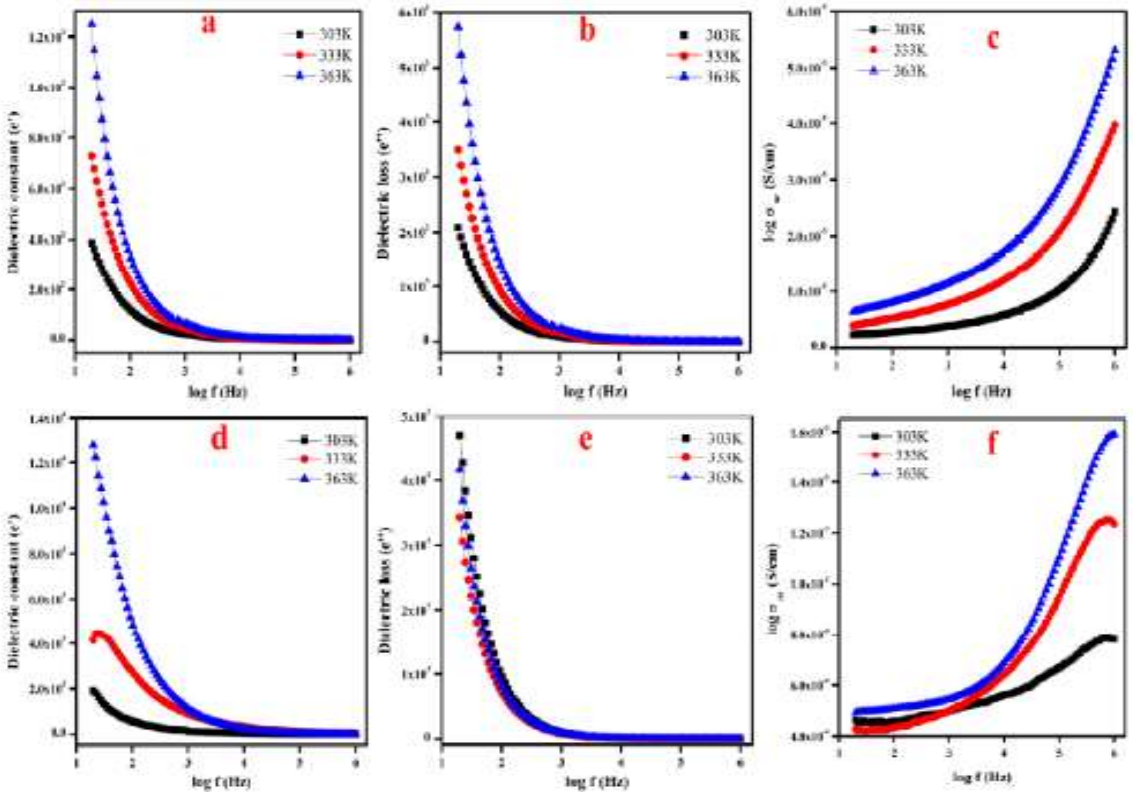

Figure 4. *Frequency dependence dielectric constant, Ac conductivity of (a),(b) &(c) Pure PPy,(d),(e) & (f) PPy-NiO nanocomposite. Reproduced from ref [26] with permission.*

Ya MaO et al. [25] prepared pristine polypyrrole using p-toluene sulfonic acid ($C_6H_4CH_3SO_3H.H_2O$, p-TSA) as a dopant and FeCl3 as the oxidant. The voltage characteristics of the PPy- NiO composite in the range of 0.0 to 3.0 V vs Li^+/Li, at a working current density of 0.1 milliamperes per square centimetre, are shown in **Figure 3**.

H. Devendrappa and colleagues [26] synthesized pure PPy and PPy-NiO nanocomposites using camphor sulfonic acid (CSA) as an anionic surfactant, FeCl3 as the oxidant and the reaction time maintained at 24 hours in an ice bath. Permittivity, dielectric dissipation, and AC conductivity were measured with varying frequencies and temperatures for both samples. The relative permittivity (ε') and dielectric dissipation factor (ε'') were calculated (**Figure 4**), showing that both decrease with increasing frequency and stabilize at higher frequencies. At lower frequencies, dipoles align with the applied field, while at higher frequencies, alignment is minimal. Higher temperatures increase permittivity and dissipation due to dipole mobility [27]. AC conductivity, determined by the equation $\sigma=2\pi f\varepsilon_o\varepsilon''$, was enhanced in PPy-NiO due to interactions between PPy and NiO nanoparticles, which reduce the conduction path and hopping distance. The current-voltage relationship is plotted (**Figure 5**) for PPy and PPy-NiO nanocomposite at room temperature. The conductivity of PPy-NiO is observed to be higher than the PPy sample. The conductivity values of PPy-NiO nanocomposite were 0.1635 S/cm, and PPy was $2.24x10^{-5}$ S/cm. The higher conductivity value in the PPy-NiO sample is due to the presence of NiO nanoparticles.

H. M. Yadav et al. [28] synthesized three nanocomposites: NiO@NMWCNT/PPy, N_2-doped multi-walled carbon nanotubes (NMWCNT), and NiO/NMWCNT composites. Raman spectra showed increased intensity, indicating structural defects in carbon. XPS spectra confirmed the presence of nickel, oxygen, carbon, and nitrogen in the composite. The uniform dispersion of NiO particles over NMWCNT enhanced the composite's electrochemical properties and specific capacitance due to increased surface area and porosity.

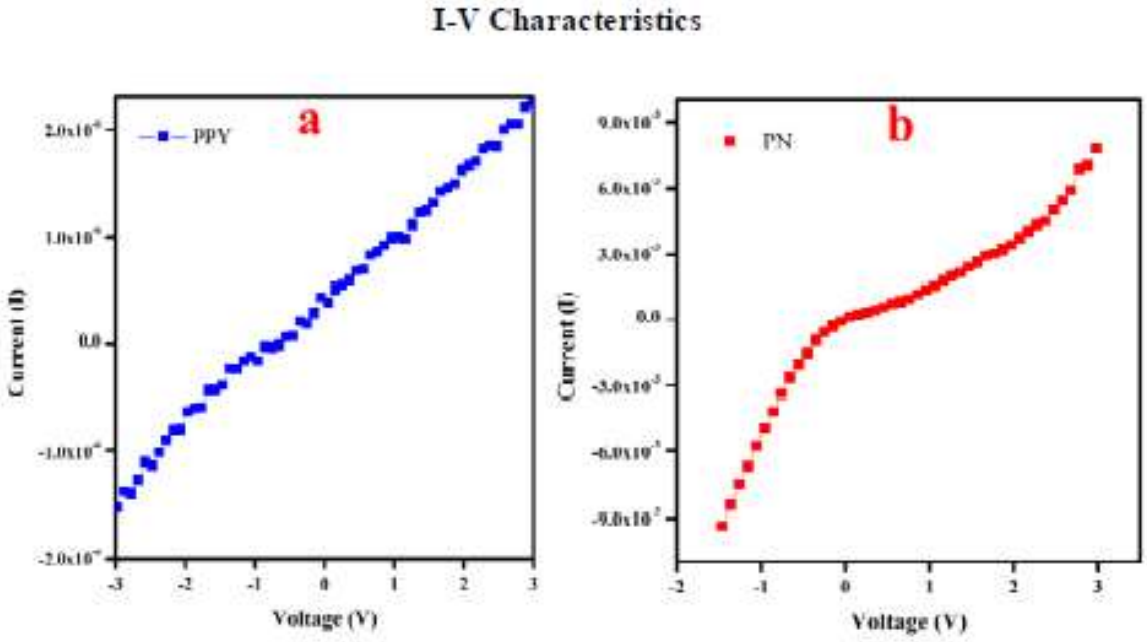

Figure 5. *I-V characteristics of (a) Pure PPy and (b) PPy- NiO nanocomposite. Reproduced from ref [26] with permission.*

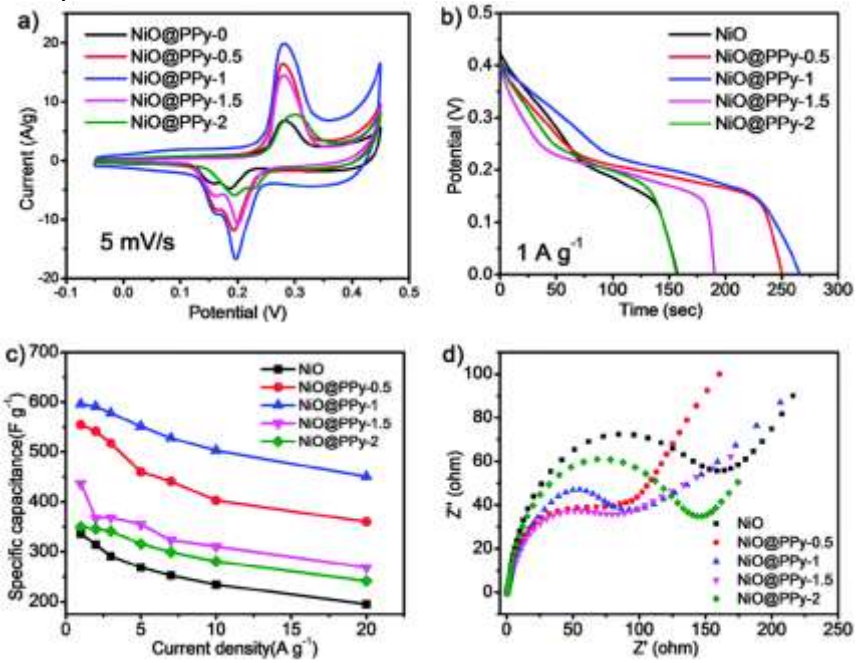

Figure 6. *a) CV curves (at 5 mV s^{-1}), b) charge-discharge curves (at 1 A g^{-1}), c) the specific capacitance and d) Nyquist plots of the hybrid electrodes (NiO@PPy-n) and the pristine electrode (NiO). Reproduced from ref [29] with permission.*

Ji et al. [29] developed a PPy-coated NiO core matrix via an in-situ method, revealing a highly porous NiO structure. The electrochemical analysis (Figure 6) demonstrated that PPy layer thickness significantly influenced the composite's electrochemical properties. Thicker PPy layers reduced specific capacitance and increased conductivity. Nyquist plots (**Figure 6d**) from EIS displayed a semicircular pattern in the high-frequency range, indicating charge transfer resistance between the electrolyte and electrode surface

4. COMPOSITES OF POLYPYRROLE -TUNGSTENOXIDE (PPy-WO_3)

Tungsten oxide (WO_3) is an oxygen-deficient oxide and often exists as a sub-stoichiometric oxide (WO_{3-x}). Due to this, it exhibits an n-type semiconductor with a wide bandgap ranging from 2.6 to 3.0 eV [30, 31].

Also, it can exist in various crystal structures like cubic, triclinic, monoclinic, orthorhombic, tetragonal and hexagonal. WO_3 often exhibits high thermal stability and promising electronic properties like superior charge transport and electron mobility. In the nanohybrid composites with PPy, the conductivity of WO_3 increases according to the oxygen ratio in the non-stoichiometric form. WO_3 is used in various forms like nanoparticles, nanodisks, nanorods, nanowires and nanofibers [32]. In any of these nano structural forms associated with PPy, it is used as gas sensors, photoelectronic devices, supercapacitors, etc.

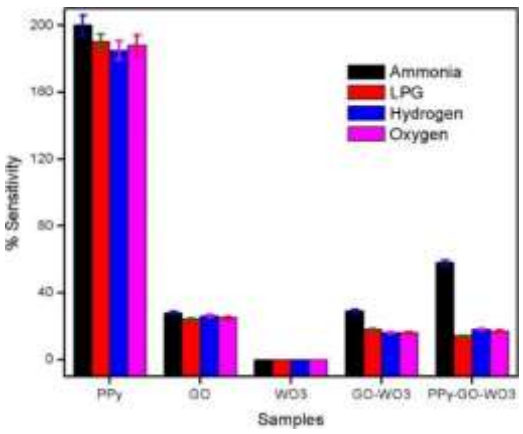

Figure 7. *Sensitivity of Sensing electrodes towards Oxygen (magenta), Hydrogen (blue), LPG (red) and Ammonia (black). Reproduced from ref [33] with permission.*

Albaris et al. [33] investigated PPy-GO-WO_3 hybrid nanocomposites for NH_3 gas sensing. PPy-GO-WO_3 selectivity towards NH_3 was tested against oxygen, hydrogen, and LPG (**Figure 7**). The hybrid nanocomposite exhibited higher sensitivity to NH_3 than individual nanostructures. For ten ppm NH_3, hybrid nanocomposites showed better performance in sensitivity, response, and recovery time (**Table 1**). Ammonia adsorption on WO_3 and subsequent electron transfer to PPy enhanced conductivity and sensitivity. WO_3 facilitated faster NH_3 desorption, improving recovery time.

Table 1. *Comparison of the sensing parameters of the fabricated electrodes towards 10 ppm of Ammonia. Reproduced from ref [33] with permission.*

Sample	Sensitivity (%)	Response Time(s)	Recovery Time(s)
PPy	200	120	–
GO	28	70	–
WO_3	0	–	–
GO–WO_3	29	60	100
PPy–GO–WO_3	58	50	120

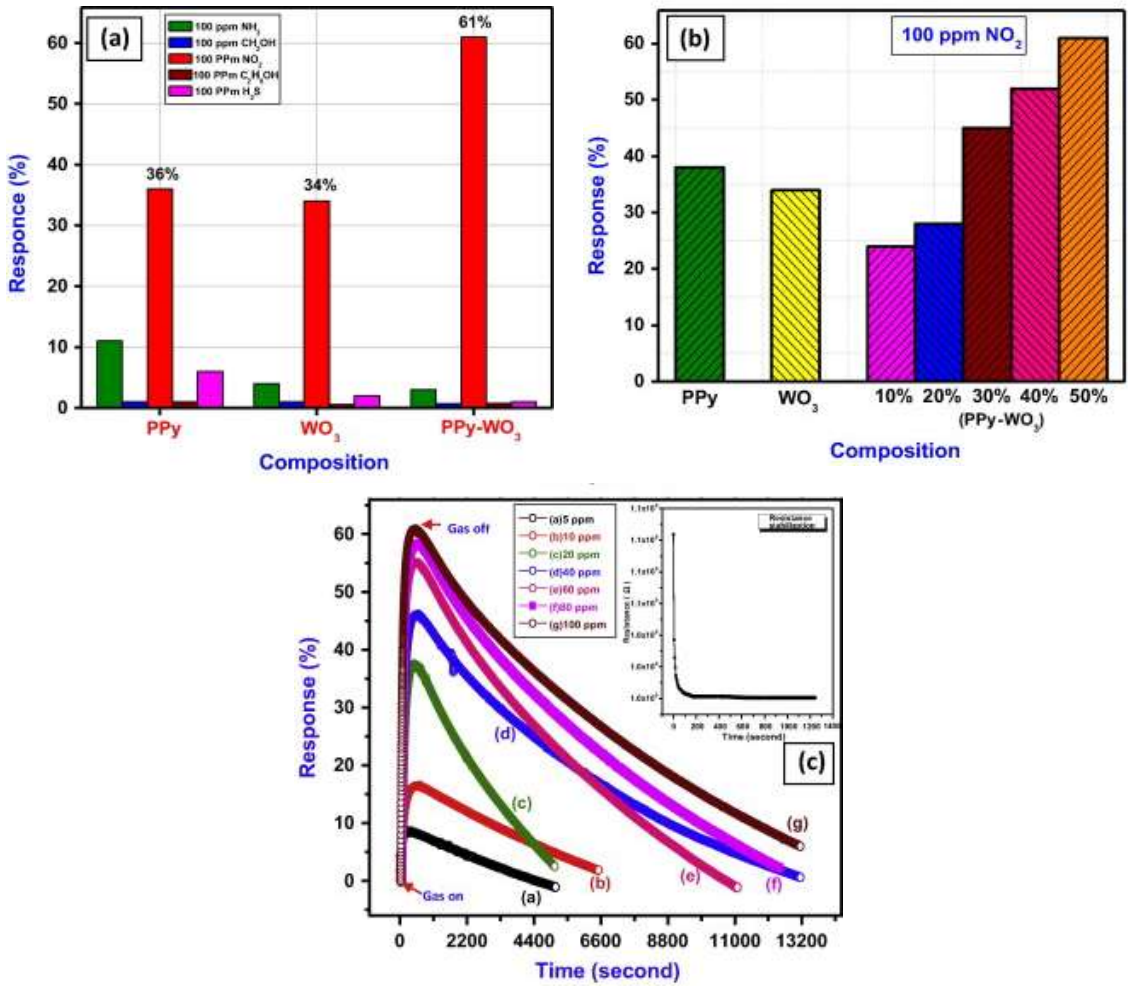

Figure 8. *Gas sensing response of PPy, WO_3 and PPy-WO_3 hybrid nanocomposite. Reproduced from ref [35] with permission.*

Mane et al. [34, 35] developed PPy/n-WO_3 composites for NO_2 gas sensing. The selectivity of PPy, WO_3, and PPy-WO_3 was tested against CH_3OH, C_2H_5OH, H_2S, NH_3, and NO_2 gases. PPy-WO_3 showed the highest response towards NO_2, with the response increasing with higher weight percentages of WO_3 (**Figure 8**). PPy-WO_3 (50%) had a response value of 61% to 100 ppm NO_2, which dropped to 8% at five ppm due to less surface area coverage by NO_2 [35]. Stability and reproducibility tests confirmed the robustness of PPy-WO_3 (50%) for NO_2 sensing at room temperature.

Hung et al.[36] synthesized Poly (4-styrene sulfonic acid) (PSSA)-doped polypyrrole (PPy)/tungsten oxide (WO_3)/reduced graphene oxide (rGO) hybrid nanocomposites *via* in situ polymerization in an aqueous solution for sensor application. The sensor showed a favorable frequency shift in response to NO exposure, with sensitivity varying between 12 Hz per ppb for 1 to 110 ppb concentrations. The frequency alteration was linear with NO concentration changes. The sensor maintained stability for over 30 days and demonstrated high repeatability at five ppb NO (**Table 2**).

In 2014, Peng et al. [37] developed a sensor for H_2S detection. They prepared a composite of WO_3/PPy on an alumina substrate. These nanocomposites were prepared using the in-situ photopolymerization method with TiO_2 as a co-photoinitiator. The sensor's reaction increased from around 9% to about 81% when the concentration of H_2S rose from a hundred parts per billion to a thousand parts per billion. The sensor's stability was considered acceptable for the initial 30-day period.

Table 2*. The sensor's reaction to different concentrations of NO. Reproduced from ref [36] with permission.*

NO Concentration (ppb)	1	5	20	50	80	110
Frequency shift (Hz)	440	707	888	1190	1691	1788
Response time (sec)	119	120	128	128	112	108
Recovery time (sec)	97	101	123	115	119	120

5. COMPOSITES OF POLYPYRROLE -ZINC OXIDE (ZnO-PPy)

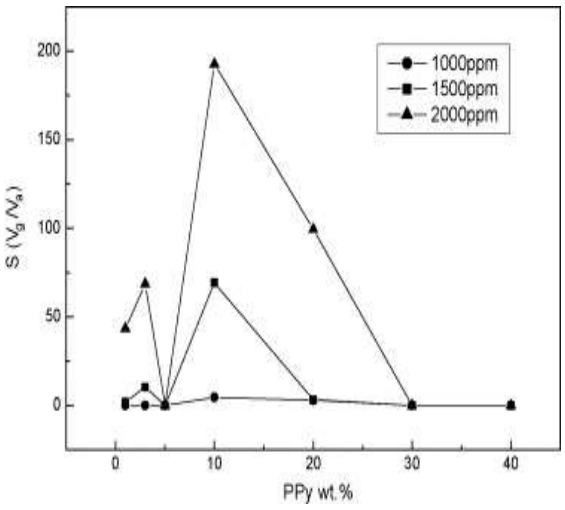

Figure 9*. The sensitivity of PPy/ZnO materials at 30°C. Reproduced from ref [39]with permission.*

Zinc oxide is a semiconductor of n-type [38] and has a hexagonal wurtzite structure, which is thermodynamically stable. Zinc oxide (ZnO) is an economical and non-toxic material with distinctive electrical, catalytic, optoelectronic, and luminescent properties. Moreover, ZnO possesses a broad energy band gap of 3.2 eV to 3.37 eV that may be influenced by the method of synthesis utilized. Zinc oxide possesses a high refractive index and thermal stability, ultraviolet protection, good transparency and high election mobility. These properties

help make nanohybrid composites with PPy for various applications.

Lina Geng et al. [39] synthesized hybrid composites of polypyrrole (PPy) and ZnO by mechanically mixing PPy in varying amounts (1%, 3%, 5%, 10%, and 40%) with ZnO. The composites were tested for gas sensitivity to NH_3, H_2S, and NO_x at 30, 60, and 90 °C. Geng et al. observed that PPy/ZnO composites with 1%, 3%, 5%, 10%, and 20% PPy content were sensitive to NO_x, while NH_3 and H_2S showed no sensitivity even at concentrations of 1000, 1500, and 2000 ppm. Both PPy (30%)/ZnO and PPy (40%)/ZnO were not susceptible to any of the gases tested (**Figure 9**). The PPy (10%)/ZnO combination exhibited the highest sensitivity to all gases under the same conditions (**Figure 10**).

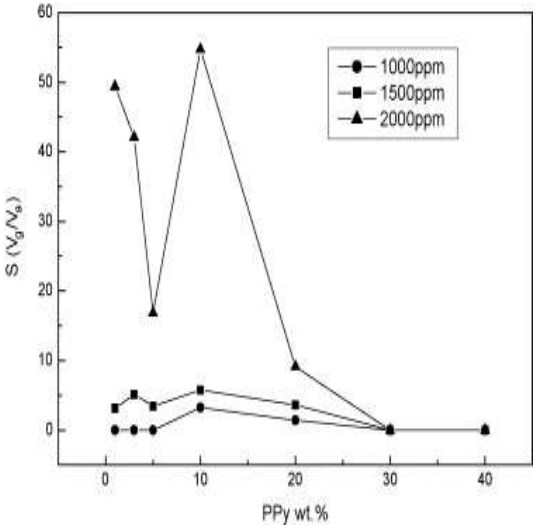

***Figure 10**. The sensitivity of PPy/ZnO materials at 60°C. Reproduced from ref [39] with permission.*

T. Fatima et al. [40] examined the DC conductivity of polypyrrole (PPy)/ZnO composites with varying ZnO concentrations (20%, 30%, 40%, and 50%) across temperatures from 302 K to 423 K. The study found that conductivity increased with temperature for pure PPy and PPy-ZnO composites, demonstrating semiconductor behavior. Conductivity at ambient temperature rose from 1.955×10^{-3} $\Omega\ m^{-1}$ for pure PPy to 5.28×10^{-3} $\Omega\ m^{-1}$ for PPy-ZnO composites, attributed to increased charge carriers due to ZnO doping. Conductivity increased steadily up to PPy-ZnO (40%) but declined at PPy-ZnO (50%) due to excessive charge carriers reducing mobility. The activation energy increased with ZnO content, except for the 40% ZnO sample, compared to pure PPy (**Figure 11**).

Khouloud Jlassi et al. [41] developed cost-effective bio-based supports by modifying polypyrrole with bentonite (B) for immobilizing metallic nanoparticles. The antibacterial efficacy was tested on A549 cells. The MTT viability assay indicated a reduction in cell viability from 80% at 0.04 mg/mL of bentonite to 50% at 0.07 mg/mL. B-PPy showed better results than pure bentonite, with the least toxicity observed in Bentonite-PPy. Using electrochemical impedance spectroscopy, the impact of PPy-ZnO on corrosion resistance was studied with varying ZnO concentrations (0 to 5 wt.%). The B-PPy/ZnO composite with four wt.% ZnO showed the highest charge transfer resistance (9.85 $M\Omega\ cm^{-2}$) compared to epoxy alone (0.213 $M\Omega\ cm^{-2}$).

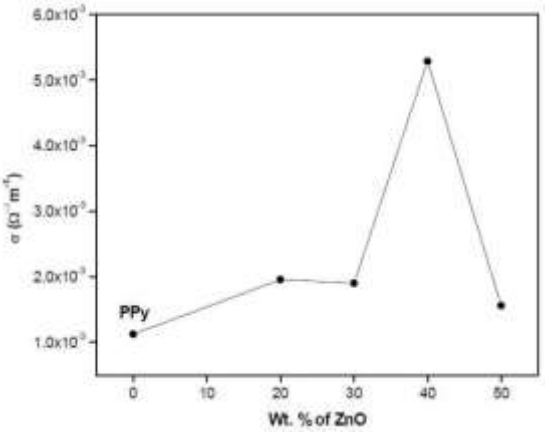

***Figure 11**. Conductivity versus ZnO concentration for PPy/ZnO composites. Reproduced from ref [40] with permission.*

Li et al. [42] synthesized PPy/ZnO nanocomposites using ZnO particles and nanosheets prepared via hydrothermal and electrospinning techniques. The ZnO nanosheet-PPy composite exhibited superior ammonia-sensing capabilities compared to pure PPy and PPy/ZnO

nanoparticle composites due to a p-n junction formation between PPy and ZnO layers and a three-dimensional porous structure facilitating ammonia diffusion. This composite also showed selective sensitivity to ammonia over other VOCs. Shimpi and colleagues found that adding dopants and metal oxides to PPy significantly enhanced its gas-sensing properties by altering its electronic and morphological characteristics [43].

Qin et al. [44] explained that adding ZnO and Camphor Sulphonic Acid to PPy increased ammonia sensitivity by 50-79% as ammonia concentration rose from 5 ppm to 120 ppm due to the formation of a p-n heterojunction in ZnO/PPy. The 1D ZnO nanostructures provided a high surface area-to-volume ratio and 15% ZnO loading on PPy-optimized transmission through the junction. Microporous structures facilitate ammonia absorption and diffusion.

Song and colleagues [45] developed PPy composites with ZnO for ammonia detection by copolymerizing Perovskite-based metal oxides with zinc stannate nanoparticles, which interacted strongly with the PPy chain. Patil et al. developed PPy/CSA-ZnO composites for NO_2 detection, achieving 80% sensitivity at 100 ppm NO_2 with a response time of 1-3 minutes and a recovery time of 24 hours at a 3.7% CSA concentration.

Sonawane et al. [46] created an LPG sensor using ZnO/PPy pellets synthesized by polymerizing pyrrole in the presence of ZnO nanoparticles via ultrasonication. The effective interconnection and narrow interface between ZnO and PPy enhanced electron transfer kinetics and gas diffusion, leading to higher gas response and lower response time than pure PPy.

6. COMPOSITES OF POLYPYRROLE -TIN OXIDE (PPy- SnO_2)

Y. Li et al. [47] researched a susceptible ammonia sensor with a detection limit below one ppm. The sensor was based on SnO_2/PPy composites, where SnO_2 sheets were arranged vertically. The composites were synthesized using a combination of vapor phase polymerization and the hydrothermal method, allowing quick preparation in only one hour. The sensor exhibited a 15% and 75% detection sensitivity in 1 and 10.7 ppm ammonia gas, respectively. Sunny and colleagues [48] also fabricated an ammonia probe with high sensitivity at ppb levels using SnO_2 nanofibers combined with PPy. This composite was prepared using the electrospinning method for SnO_2 and vapor phase polymerization of pyrrole. The detector exhibited a response (%) that spanned from 57% to 182.2% for exceedingly small amounts of ammonia, ranging from 100 parts per million (ppm) to 2.5 ppm, respectively. The porous microstructure of SnO_2, along with its Debye length and particle size, facilitated the absorption and desorption kinetics of ammonia molecules.

Mude and colleagues [49] conducted a study and found that a composite made of SnO_2 and polypyrrole (PPy) can detect 100 ppm concentration of CO_2 with 65% sensitivity. The composite material displays a distinctive character where a heterojunction at a particular site is generated between two dissimilar materials with distinct chemical compositions. The metal oxide (n-type) nanoparticles and PPy (p-type) composites combine to form a composite material that generates an n-p heterojunction. The presence of this junction leads to the development of a strong depletion layer near the junction. This depletion layer arises from the transport of electrons and gaps in divergent directions until a state of balance is achieved. The impedance characteristics of n-p junctions within these composites can be modulated by manipulating the composition of either oxidizing or reducing agents. For reducing gases such as NH_3, the deprotonation process dramatically reduces the hole density in the PPy matrix. This results in an expansion of the width of the depletion region, causing an increase in the contrast between the base impedance of the

detector when exposed to air/nitrogen and the resistance observed when exposed to target analytes. It was also suitable for detecting low ppm CO_2 concentrations. However, it has a long response time of 2 minutes and a recovery time of 1 minute.

7. COMPOSITES OF POLYPYRROLE -TITANIUM OXIDE (PPy–TiO_2)

Titanium oxides—rutile, anatase, and brookite—feature an octahedral structure with titanium bonded to six oxide anions [50]. Rutile has a tetragonal structure, while anatase and brookite are orthorhombic. Titanium oxides exhibit n-type semiconductor behavior with a band gap of 3.2 − 3.35 eV, similar to ZnO. When combined with polypyrrole (PPy), TiO_2 enhances PPy's conductivity by forming p-n junctions, both externally and within the composite. This interaction with oxygen results in significant charge exchange and impacts the depletion regions of the p-n junctions. Consequently, the conductivity of PPy/TiO_2 nanocomposites increases approximately 20-fold compared to unaltered PPy [50].

Jiang (2007) [51] developed a TiO_2/PPy composite for NH_3 sensing using a self-assembled structure with PSS/PDDA layers. This method facilitated PPy growth around TiO_2 nanoparticles deposited on the quartz substrate.

Sun et al. [52] synthesized a PPy/TiO_2 composite doped with Pd for hydrogen sensing, achieving high sensitivity (6%-26%) for H_2 concentrations from 0.005% to 2.5% vol. The composite demonstrated selective sensitivity to H_2 over CO_2 and H_2S due to palladium's catalytic reduction of H_2 molecules, improving the composite's hydrogen sensitivity.

Debabrata Nandi et al. [53] prepared and characterized titania-doped iron oxide polypyrrole composites. They synthesized Fe(III)-Ti(IV) oxide (NITO) nanocomposites by reacting $TiCl_4$ with ferric chloride and NaOH, forming a yellow-brown precipitate. The resulting PPy/NITO nanocomposites were characterized using XRD, confirming NITO's incorporation into the polymer matrix. The conductivity decreased with increasing NITO content, attributed to the expansion of the bipolaron energy gap. Pristine PPy showed lower conductivity than composites, and the composite with a higher amount (0.25 gm) of NITO showed the lowest conductivity. The polymer chain continuity was affected by higher NITO content.

Gao et al. [54, 55] deposited PPy onto TiO_2 nanotubes *via* electrochemical methods, enhancing the nanotubes surface area and electronic conductance.

8. COMPOSITES OF POLYPYRROLE WITH OTHER METAL OXIDES

8.1. With Manganese Oxide (PPy-MnO_2)

Manganese Dioxide exists in several polymorphs. It crystallizes mainly in a rutile structure called B-MnO_2 with three coordinate oxide and octahedral metal centres [56]. MnO_2 is considered nonstoichiometric and deficient in oxygen; the α polymorph of MnO_2 has an open structure with channels that can accommodate metal ions of Barium or silver. MnO_2 has a low electrical conductivity (10^{-5} to 10^{-6} S/cm) and a low ionic diffusion constant (~10^{-13} cm^2 /Vs).

Ji et al. [57] prepared a coating of the composite of PPy/MnO_2 where nanotubes of PPy surrounded MnO_2. This coating was observed to have high capacity and stability. Similarly, the chemical oxidation of Pyrrole was carried out by Šešelj et al. [58] with $KMnO_4$ converted into MnO_2/PPy composites. This composite was more stable even at low electrode potentials.

R. K. Sharma et al. [59] prepared PPy by electrodeposition process in the presence of $MnSO_4$. This Reaction converted the porous PPy matrix along with MnO_2 particles. This porosity created a large active surface area that was useful and increased electronic conductivity. The interlinking between the porous matrix of PPy and MnO_2 particles increased the stability of the composite. Malook et al.

[60] reported that forming p-n junctions on the enhanced surface is responsible for ammonia sensing on MnO_2/PPy composites compared to pristine PPy.

8.2. Ruthenium Oxide (PPy-RuO_2)

J. F. Zang et al. [61] showed that the capacitance increased three times when nano cones of PPy were deposited by a layer of RuO_2 as compared to uncoated cones of PPy due to its particle morphology and creation of a sizeable interfacial contact area.

8.3. Cerium Oxide (PPy-CeO_2)

Wang et al. [62] deposited CeO_2 particles on PPy by a chemical deposition. They used surface-functionalized particles of CeO_2. This process improved electronic conductance as compared to plain PPy.

8.4. Iron Oxide (Fe_2O_3)

Tang et.al [63] developed Honey Camblite Fe_2O_3 (Hematite) nanoflakes on nickel foam with branched PPy nano leaves. These composites showed high stability and capacity.

8.5. Molybdenum Oxide (MoO_3)

F. Wang et al. [64] improved the capacity of the PPy by preparing composites with hollow MoO_3 nanotubes by a coating method. The benefit is also reflected in structural stability.

8.6. Bismuth Oxide (Bi_2O_3)

Chowdhary et al. [65] conducted a study to investigate the gas-sensing properties of composites containing binary metal oxides in the presence of LPG gas. The composites were denoted as PPy-Bi_2O_3-MO_x, where MO_x represents ZrO_2, Ag_2O, and TiO_2. The composite (PPy-Bi_2O_3-Ag_2O) exhibited the highest selectivity towards LPG gas. A linear increase in response (%) was observed for all the compounds, showing an elevation in LPG concentration up to five hundred parts per million. The optimal temperature for gas sensing was found to be 350 K. The adsorption of gas molecules on the surface of the composites was due to internal vibrations of the gas molecules, which occurred at higher temperatures.

9. COMPOSITES OF POLYPYRROLE WITH NANO YTTRIUM OXIDE (PPy-Y_2O_3)

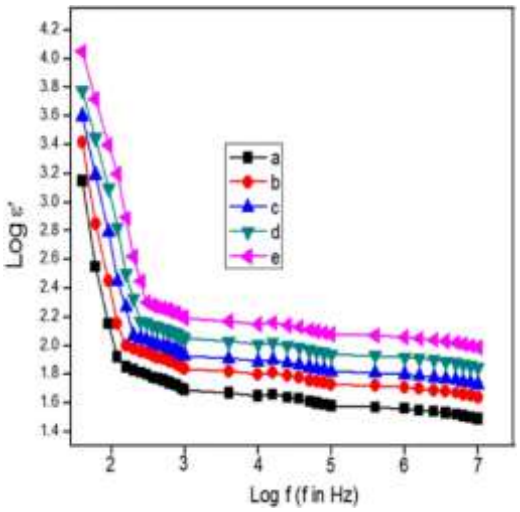

Figure 12. *Variation in dielectric constant vs frequency for (a) PPy, (b) PPy-DBSA, (c) 2% Y_2O_3, (d) 4% Y_2O_3 and (e) 8% Y_2O_3 in PPy-DBSA. Reproduced from ref [67] with permission.*

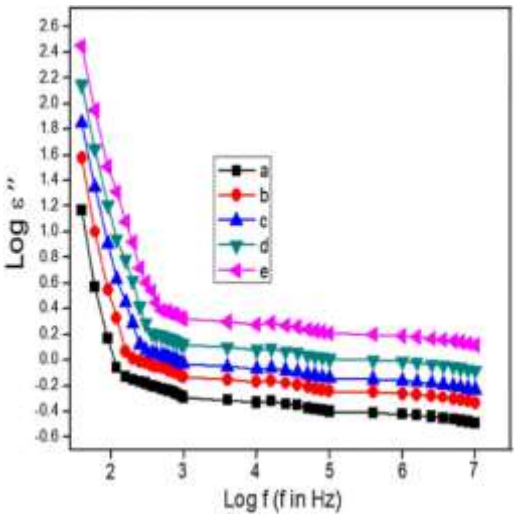

Figure 13. *Variation in dielectric constant vs frequency for (a) PPy, (b) PPy-DBSA, (c) 2% Y_2O_3, (d) 4% Y_2O_3 and (e) 8% Y_2O_3 in PPy-DBSA. Reproduced from ref [67]with permission.*

Yttrium Oxide is a well-known body-centred cubic material [66]. Yttrium ions occupy two distinct sites: eight sites with

octahedral coordination and C_{3i} point symmetry and 24 sites with prismatic coordination and C_2 symmetry. Six oxygen ions surround each yttrium ion. Yttria has a band gap of around 6.0 eV [66]. Yttria is widely used in lasers, gas lighting, dental ceramics, microwave filters and super-conductors.

Muhammad Irfan et al. [67] synthesized polypyrrole (PPy) by chemical polymerization using APS, DBSA, HCl and Y_2O_3 powder. Dielectric measurements (Keithley 2400) demonstrated (Figures 12 & 13) that the dielectric constant (ε') decreased with increasing frequency and Y_2O_3 content, while higher ε' values were observed at lower frequencies due to polarization and charge movement. The dielectric loss (ε") increased with Y_2O_3 content, decreasing with higher frequencies due to less energy dissipation.

A comparative table of various Conducting polymer/Metal oxide nano-composites tested for gas sensing applications for various gases like NH_3, NO_2, LPG, H_2S, etc. are presented in Table 3. This table indicates that the nanocomposites of PANi/metal oxides and PPy/metal oxides have good gas-sensing properties.

***Table 3**. Comparative studies of various Conducting Polymers/Metal oxides hybrid composites used in gas sensors [68]*

Polymer	Metal Oxides	Target Gas	Concentration (ppm)	Response	Response/Recovery time (sec)	Temperature °C
PANi	TiO_2	NH_3	23	1.67	18 ~58	25
		CO	140	~1.9	-	-
		NH_3	50 ppt	0.4%		RT
	SnO_2	NH_3	100	-	15 ~80	
		NO_2	50 ppb	-	5 ~15 mins	25
	ZnO	NH_3	20	14%	< 35	300K
	WO_3	NH_3	5	24%	136 ~137	RT
		NO_2	100	~40%		
PANi: PSS	Fe_2O_3	NO_2	0.5	~8%		RT
PPy	SnO_2	NH_3	10.7	75%	259 ~468	RT
	ZnO	LPG	1400	32.5%	4 ~40 mins	RT
		NH_3	0.5	21%	256 ~370	RT
	TiO_2	LPG	1040	55%	112 ~131	RT
	WO_3	H_2S	1	83%	6 ~210 mins	RT
		NO_2	100	61%		38
PPy-DBSA	WO_3	NO_2	100	72%	288 ~5990	38
PT	SnO_2	NO_2	100	3.69		90
	WO_3	H_2S	100	1.35	< 15	70
PEDOT: PSS	TiO_2	NO_2	0.005			RT
	WO_3	NO_2	0.05	~1.2	45.1 ~88.7	RT

10. CONCLUSION

In summary, conducting polymers such as PPy and metal oxides show significant improvements in electrical conductivity, stability, and performance across various applications. The hybrid nanocomposites enhance supercapacitance, electro-chromism, and gas sensing properties. Future research should optimize synthesis methods and explore new applications for these advanced materials.

FINANCIAL ASSISTANCE

The scientists have not obtained any monetary assistance for conducting, composing, and disseminating this research.

STATEMENT OF CONFLICTING INTERESTS

The authors declare that they have no conflicts of interest.

AUTHOR CONTRIBUTION

"All authors contributed to the study conception and design. Nandini V. Iyer: conceptualization, methodology, formal analysis, writing-original data, Ganesh L. Agawane: conceptualization, methodology, formal analysis, writing-review and editing, Chandan Patel: conceptualization, methodology, formal analysis, writing-review and editing, Jayant Kher: conceptualization, methodology, formal analysis, writing-review and editing and Shekhar Bhame; conceptualization, methodology, formal analysis, writing-review and editing. All authors read and approved the final manuscript."

REFERENCES

1. Walatka, V. V., Labes, M. M., Perlstein, J. H., "Polysulfur Nitride—a One-Dimensional Chain with a Metallic Ground State", *Phys. Rev. Lett.*, 31 (1973) 1139–1142. https://doi.org/10.1103/PhysRevLett.31.1139.
2. Zaumseil, J., "P3HT and Other Polythiophene Field-Effect Transistors, Advances in Polymer Science", Springer Berlin Heidelberg, (2014) 107–137. https://doi.org/10.1007/12_2014_279.
3. Sharma, S., Sudhakara, P., Omran, A. A. B., Singh, J., Ilyas, R. A., "Recent Trends and Developments in Conducting Polymer Nanocomposites for Multifunctional Applications", *Polymers (Basel)*, 13 (2021) 2898. https://doi.org/10.3390/polym13172898.
4. Jamjoum, H. A. A., Umar, K., Adnan, R., Razali, M. R., Mohamad Ibrahim, M. N., "Synthesis, Characterization, and Photocatalytic Activities of Graphene Oxide/metal Oxides Nanocomposites: A Review", *Front. Chem.*, 9 (2021). https://doi.org/10.3389/fchem.2021.752276.
5. Nguyen, D., Yoon, H., "Recent Advances in Nanostructured Conducting Polymers: from Synthesis to Practical Applications", *Polymers (Basel)*, 8 (2016) 118. https://doi.org/10.3390/polym8040118.
6. Holze, R., Wu, Y. P., "Intrinsically conducting polymers in electrochemical energy technology: Trends and progress", *Electrochim. Acta*, 122 (2014) 93–107. https://doi.org/10.1016/j.electacta.2013.08.100.
7. Ranjbar, M., Yousefi, M., "Sonochemical Synthesis and Characterization of a Nano-Sized Lead (II) Coordination Polymer; A New Precursor for the Preparation of PbO Nanoparticles", *Ultrasonics Sonochemistry*, 20 (2016) 1254-1260.
8. Hu, C., Li, T., Yin, H., Hu, L., Tang, J., Ren, K., "Preparation and corrosion protection of three different acids doped polyaniline/epoxy resin composite coatings on carbon steel", *Colloids Surf. A Physicochem. Eng. Asp.*, 612 (2021) 126069. https://doi.org/10.1016/j.colsurfa.2020.126069.
9. Sathiyanarayanan, S., Azim, S., Venkatachari, G., "Preparation of polyaniline–TiO_2 composite and its comparative corrosion protection performance with polyaniline", *Synth. Met.*, 157 (2007) 205–213. https://doi.org/10.1016/j.synthmet.2007.01.012.
10. Castagno, K. R. L., Azambuja, D. S., Dalmoro, V., "Polypyrrole electropolymerized on aluminium alloy 1100 doped with oxalate and tungstate anions", *J. Appl. Electrochem.*, 39 (2009) 93–100. https://doi.org/10.1007/s10800-008-9640-1.
11. Liras, M., Barawi, M., de la Peña O'Shea, V. A., "Hybrid materials based on conjugated polymers and inorganic semiconductors as photocatalysts: from environmental to energy applications", *Chem. Soc. Rev.*, 48 (2019) 5454–5487. https://doi.org/10.1039/C9CS00377K.
12. Gao, F., Hou, X., Wang, A., Chu, G., Wu, W., Chen, J., Zou, H., "Preparation of polypyrrole/TiO_2 nanocomposites with enhanced photocatalytic performance", *Particuology*, 26 (2016) 73–78. https://doi.org/10.1016/j.partic.2015.07.003.
13. Meng, Z., Mirica, K. A., "Covalent organic frameworks as multifunctional materials for chemical detection", *Chem. Soc. Rev.*, 50 (2021) 13498–13558. https://doi.org/10.1039/D1CS00600B.
14. De Alvarenga, G., Hryniewicz, B. M., Jasper, I., Silva, R.J., Klobukoski, V., Costa, F. S., Cervantes, T. N. M., Amaral, C. D. B., Schneider, J. T., Bach-Toledo, L., Peralta-Zamora, P., Valerio, T. L., Soares, F., Silva, B. J. G., Vidotti, M., "Recent trends of micro and nanostructured conducting polymers in health and environmental applications", *Journal of Electroanalytical Chemistry*, 879 (2020) 114754. https://doi.org/10.1016/j.jelechem.2020.114754.
15. Anna B., Neerooa B. N. H. M., Hu Y., Ooi L., Shameli K., Chew J., Teow S., "Development of FDA-Approved Antibacterial Metal and Metal Oxide Nanoparticles: An Update", *Int. J. Nanosc. Nanotechnol.*, 19 (2023) 209–235. https://doi.org/10.22034/ijnn.2023.1978122.2311.
16. Hao L., Dong C., Zhang L., Zhu K., Yu D., "Polypyrrole Nanomaterials: Structure, Preparation and Application", *Polymers (Basel)*, 14 (2022) 5139. https://doi.org/10.3390/polym14235139.

17. Le T., Yoon H., "Fundamentals of Conjugated Polymer Nanostructures. Conjugated Polymer Nanostructures for Energy Conversion and Storage Applications", Wiley, (2021) 1–42. https://doi.org/10.1002/9783527820115.ch1.
18. Pang A.L., Arsad A., Ahmadipour M., "Synthesis and factor affecting on the conductivity of polypyrrole: a short review", *Polym. Adv. Technol.*, 32 (2021) 1428–1454. https://doi.org/10.1002/pat.5201.
19. Kiani, M. S., Mitchell, G.R., "The role of the counter-ion in the preparation of polypyrrole films with enhanced properties using a pulsed electrochemical potential", *Synth. Met.*, 48 (1992) 203–218. https://doi.org/10.1016/0379-6779(92)90062-N.
20. Namsheer K., Rout, C. S., "Conducting polymers: a comprehensive review on recent advances in synthesis, properties and applications", *RSC Adv.*, 11 (2021) 5659–5697. https://doi.org/10.1039/D0RA07800J.
21. Chen, Y., Zhao, Z., Zhang, C., "Structural and electrochemical study of polypyrrole/ZnO nanocomposites coating on nickel sheet synthesized by electrochemical method", *Synth. Met.*, 163 (2013) 51–56. https://doi.org/10.1016/j.synthmet.2012.12.013.
22. Khodair, Z. T., Ibrahim, N. M., Kadhim, T. J., Mohammad, A. M., "Synthesis and characterization of nickel oxide (NiO) nanoparticles using an environmentally friendly method, and their biomedical applications", *Chem. Phys. Lett.*, 797 (2022) 139564. https://doi.org/10.1016/j.cplett.2022.139564.
23. Inamdar, H. K., Ambikaprasad, M. V. N., Sasikal, M., "Synthesis and characterization of polypyrrole/NiO doped Nanocomposites (NCs) for Dielectric studies", *Materials Today: Proceedings*, 5 (2018) 22652-22656. http://dx.doi.org/10.1016/j.matpr.2018.06.640.
24. Inamdar, H. K., Sridhar, B. C., Sasikal, M., Ambika Prasad, M. V. N., "Structural and Optical Properties of Polypyrrole/NiO Doped Nanocomposites", *Journal of Nanoscience and Technology*, 4 (2018) 400–401. https://doi.org/10.30799/jnst.112.18040308.
25. Mao, Y., Kong, Q., Guo, B., Shen, L., Wang, Z., Chen, L., "Polypyrrole–NiO composite as high-performance lithium storage material", *Electrochim. Acta*, 105 (2013) 162–169. https://doi.org/10.1016/j.electacta.2013.04.086.
26. Vijeth, H., Kumar, S. P. A., Yesappa, L., Niranjana, M., Vandana, M., Devendrappa, H., "Influence of nickel oxide nanoparticle on the structural, electrical and dielectric properties of polypyrrole nanocomposite", in: *AIP Conference Proceedings*. AIP Publishing, (2019) 150029. https://doi.org/10.1063/1.5122578.
27. Murugavel, S., Malathi, M., "Structural, photoconductivity, and dielectric studies of polythiophene-tin oxide nanocomposites", *Mater. Res. Bull.*, 81 (2016) 93–100. https://doi.org/10.1016/j.materresbull.2016.05.004.
28. Yadav, H. M., Ramesh, S., Kumar, K. A., Shinde, S., Sandhu, S., Sivasamy, A., Shrestha, N.K., Kim, H. S., Kim, H. -S., Bathula, C., "Impact of polypyrrole incorporation on nickel oxide@multi walled carbon nanotube composite for application in supercapacitors", *Polym. Test.*, 89 (2020) 106727. https://doi.org/10.1016/j.polymertesting.2020.106727.
29. Ji, W., Ji, J., Cui, X., Chen, J., Liu, D., Deng, H., Fu, Q., "Polypyrrole encapsulation on flower-like porous NiO for advanced high-performance supercapacitors", *Chemical Communications*, 51 (2015) 7669–7672. https://doi.org/10.1039/c5cc00965k.
30. Deepa, M., Sharma, R., Basu, A., Agnihotry, S. A., "Effect of oxalic acid dihydrate on optical and electrochemical properties of sol–gel derived amorphous electrochromic WO_3 films", *Electrochim. Acta*, 50 (2005) 3545–3555. https://doi.org/10.1016/j.electacta.2005.01.008.
31. Cheng, W., Baudrin, E., Dunn, B., Zink, J. I., "Synthesis and electrochromic properties of mesoporous tungsten oxide", *J. Mater. Chem.*, 11 (2001) 92–97. https://doi.org/10.1039/b003192p.
32. Hariharan, V., Gnanavel, B., Sathiyapriya, R., Aroulmoji, V., "A Review on Tungsten Oxide (WO_3) and their Derivatives for Sensor Applications", *International Journal of Advanced Science and Engineering*, 5 (2019) 1163–1168. https://doi.org/10.29294/IJASE.5.4.2019.1163-1168.
33. Albaris, H., Karuppasamy, G., "Investigation of NH_3 gas sensing behavior of intercalated PPy–GO–WO3 hybrid nanocomposite at room temperature", *Materials Science and Engineering: B*, 257 (2020). https://doi.org/10.1016/j.mseb.2020.114558.
34. Navale, S. T., Mane, A. T., Chougule, M. A., Sakhare, R. D., Nalage, S. R., Patil, V. B., "Highly selective and sensitive room temperature NO_2 gas sensor based on polypyrrole thin films", *Synth. Met.*, 189 (2014) 94–99. https://doi.org/10.1016/j.synthmet.2014.01.002.
35. Mane, A. T., Navale, S. T., Sen, S., Aswal, D. K., Gupta, S. K., Patil, V. B., "Nitrogen dioxide (NO_2) sensing performance of p-polypyrrole/n-tungsten oxide hybrid nanocomposites at room temperature", *Org. Electron.*, 16 (2015) 195–204. https://doi.org/10.1016/j.orgel.2014.10.045.
36. Hung, T. T., Chung, M. H., Chiu, J. J., Yang, M. W., Tien, T. N., Shen, C. Y., "Poly (4-styrenesulfonic acid) doped polypyrrole/tungsten oxide/reduced graphene oxide nanocomposite films based surface acoustic wave sensors for NO sensing behavior", *Org. Electron.*, 88 (2021). https://doi.org/10.1016/j.orgel.2020.106006.
37. Su, P. -G., Peng, Y. -T., "Fabrication of a room-temperature H_2S gas sensor based on PPy/WO_3 nanocomposite films by in-situ photopolymerization", *Sens. Actuators B Chem.*, 193 (2014) 637–643. https://doi.org/10.1016/j.snb.2013.12.027.

38. Özgür, Ü., Alivov, Ya. I., Liu, C., Teke, A., Reshchikov, M. A., Doğan, S., Avrutin, V., Cho, S. -J., Morkoç, H., "A comprehensive review of ZnO materials and devices", *J. Appl. Phys.*, 98 (2005). https://doi.org/10.1063/1.1992666.
39. Geng, L., Zhao, Y., Huang, X., Wang, S., Zhang, S., Huang, W., Wu, S., "The preparation and gas sensitivity study of polypyrrole/zinc oxide", *Synth. Met*., 156 (2006) 1078–1082. https://doi.org/10.1016/j.synthmet.2006.06.019.
40. Fatima, T., Sankarappa, T., Ramanna, R., "DC Conductivity Studies of PPy/ZnO Composites", *Research Journal of Material Sciences*, 3 (2015) 1-5. www.isca.in.
41. Jlassi, K., Sliem, M. H., Benslimane, F. M., Eltai, N. O., Abdullah, A. M., "Design of hybrid clay/ polypyrrole decorated with silver and zinc oxide nanoparticles for anticorrosive and antibacterial applications", *Prog. Org. Coat.*, 149 (2020) 105918. https://doi.org/10.1016/j.porgcoat.2020.105918.
42. Li, Y., Jiao, M., Yang, M., "In-situ grown nanostructured ZnO via a green approach and gas sensing properties of polypyrrole/ZnO nanohybrids", *Sens. Actuators B Chem.*, 238 (2017) 596–604. https://doi.org/10.1016/j.snb.2016.07.089.
43. Jain, S., Karmakar, N., Shah, A., Kothari, D. C., Mishra, S., Shimpi, N. G., "Ammonia detection of 1-D ZnO/polypyrrole nanocomposite: Effect of CSA doping and their structural, chemical, thermal and gas sensing behavior", *Appl. Surf. Sci.*, 396 (2017) 1317–1325. https://doi.org/10.1016/j.apsusc.2016.11.154.
44. Qin, Y., Zhang, T., Cui, Z., "Core-shell structure of polypyrrole grown on $W_{18}O_{49}$ nanorods for high performance gas sensor operating at room temperature", *Org. Electron.*, 48 (2017) 254–261. https://doi.org/10.1016/j.orgel.2017.06.014.
45. Song, P., Wang, Q., Yang, Z., "Ammonia gas sensor based on PPy/$ZnSnO_3$ nanocomposites", *Mater. Lett.*, 65 (2011) 430–432. https://doi.org/10.1016/j.matlet.2010.10.087.
46. Barkade, S. S., Pinjari, D. V., Singh, A. K., Gogate, P.R., Naik, J. B., Sonawane, S. H., Ashokkumar, M., Pandit, A. B., "Ultrasound Assisted Miniemulsion Polymerization for Preparation of Polypyrrole–Zinc Oxide (PPy/ZnO) Functional Latex for Liquefied Petroleum Gas Sensing", *Ind. Eng. Chem. Res.*, 52 (2013) 7704–7712. https://doi.org/10.1021/ie301698g.
47. Li, Y., Ban, H., Yang, M., "Highly sensitive NH_3 gas sensors based on novel polypyrrole-coated SnO_2 nanosheet nanocomposites", *Sens. Actuators B Chem.*, 224 (2016) 449–457. https://doi.org/10.1016/j.snb.2015.10.078.
48. Beniwal, A., Sunny, "Electrospun SnO2/PPy nanocomposite for ultra-low ammonia concentration detection at room temperature", *Sens. Actuators B Chem.*, 296 (2019) 126660. https://doi.org/10.1016/j.snb.2019.126660.
49. Mude, B. M., Raulkar, K. B., "Study of CO_2 gas detection by multilayer SnO_2-ZnO-PPy sensor," *Vidyabharati International Interdisciplinary Research Journal*, 12 (2017) 143–148.
50. Duong, H.N., Nguyen, T. -P., Nguyen, T. T., "Effect of TiO_2 anatase nanocrystallite on electrical properties of PPy/TiO_2 nanocomposite", *Communications in Physics*, 28 (2018) 87. https://doi.org/10.15625/0868-3166/28/1/11036.
51. Tai, H., Jiang, Y., Xie, G., Yu, J., Zhao, M., "Self-assembly of TiO_2 /polypyrrole nanocomposite ultrathin films and application for an NH_3 gas sensor", *Int. J. Environ. Anal. Chem.*, 87 (2007) 539–551. https://doi.org/10.1080/03067310701272954.
52. Zou, Y., Wang, Q., Jiang, D., Xiang, C., Chu, H., Qiu, S., Zhang, H., Xu, F., Sun, L., Liu, S., "Pd-doped TiO_2@polypyrrole core-shell composites as hydrogen-sensing materials", *Ceram. Int.*, 42 (2016) 8257–8262. https://doi.org/10.1016/j.ceramint.2016.02.038.
53. Nandi, D., Ghosh, A. K., Gupta, K., De, A., Sen, P., Duttachowdhury, A., Ghosh, U. C., "Polypyrrole-titanium (IV) doped iron (III) oxide nanocomposites: Synthesis, characterization with tunable electrical and electrochemical properties", *Mater. Res. Bull.*, 47 (2012) 2095–2103. https://doi.org/10.1016/j.materresbull.2012.03.040.
54. Gao, Y., Ding, K., Xu, X., Wang, Y., Yu, D., "PPy film/TiO_2 nanotubes composite with enhanced supercapacitive properties", *RSC Adv.*, 4 (2014) 27130–27134. https://doi.org/10.1039/C4RA03014A.
55. Gao, Y., Wang, Y., Xu, X., Ding, K., Yu, D., "Synthesis of polypyrrole–titanium dioxide brush-like nanocomposites with enhanced supercapacitive performance", *RSC Adv.*, 4 (2014) 63719–63724. https://doi.org/10.1039/C4RA10680F.
56. Birgisson, S., Saha, D., Iversen, B. B., "Formation Mechanisms of Nanocrystalline MnO_2 Polymorphs under Hydrothermal Conditions", *Cryst. Growth Des.*, 18 (2018) 827–838. https://doi.org/10.1021/acs.cgd.7b01304.
57. Ji, J., Zhang, X., Liu, J., Peng, L., Chen, C., Huang, Z., Li, L., Yu, X., Shang, S., "Assembly of polypyrrole nanotube@MnO_2 composites with an improved electrochemical capacitance", *Materials Science and Engineering: B*, 198 (2015) 51–56. https://doi.org/10.1016/j.mseb.2015.04.004.
58. Šešelj, N., Karakterizacija pseudokapacitivnih svojstava kemijski priređenog MnO_2 te kompozita MnO_2/polipirol, *Kemija u Industriji*, 65 (2016) 127–136. https://doi.org/10.15255/KUI.2015.009.

59. Sharma, R. K., Rastogi, A. C., Desu, S. B., "Manganese oxide embedded polypyrrole nanocomposites for electrochemical supercapacitor", *Electrochim. Acta*, 53 (2008) 7690–7695. https://doi.org/10.1016/j.electacta.2008.04.028.
60. Malook, K., Khan, H., Shah, M., Haque, I., "Highly selective and sensitive response of Polypyrrole–MnO_2 based composites towards ammonia gas", *Polym. Compos.*, 40 (2019) 1676–1683. https://doi.org/10.1002/pc.24917.
61. Zang, J., Bao, S. -J., Li, C. M., Bian, H., Cui, X., Bao, Q., Sun, C. Q., Guo, J., Lian, K., "Well-Aligned Cone-Shaped Nanostructure of Polypyrrole/RuO_2 and Its Electrochemical Supercapacitor", *The Journal of Physical Chemistry C*, 112 (2008) 14843–14847. https://doi.org/10.1021/jp8049558.
62. Wang, X., Wang, T., Liu, D., Guo, J., Liu, P., "Synthesis and Electrochemical Performance of CeO_2/PPy Nanocomposites: Interfacial Effect", *Ind. Eng. Chem. Res.*, 55 (2016) 866–874. https://doi.org/10.1021/acs.iecr.5b03891.
63. Tang, P. -Y., Han, L. -J., Genç, A., He, Y. -M., Zhang, X., Zhang, L., Galán-Mascarós, J. R., Morante, J. R., Arbiol, J., "Synergistic effects in 3D honeycomb-like hematite nanoflakes/branched polypyrrole nanoleaves heterostructures as high-performance negative electrodes for asymmetric supercapacitors", *Nano Energy*, 22 (2016) 189–201. https://doi.org/10.1016/j.nanoen.2016.02.019.
64. Wang, F., Liu, Z., Wang, X., Yuan, X., Wu, X., Zhu, Y., Fu, L., Wu, Y., "A conductive polymer coated MoO_3 anode enables an Al-ion capacitor with high performance", *J. Mater. Chem. A Mater.*, 4 (2016) 5115–5123. https://doi.org/10.1039/C6TA01398H.
65. Choudhary, A. R., Waghuley, S. A., "LPG sensing application of PPy based nanocomposites at low operable temperature", *Mater. Lett.*, 205 (2017) 36–39. https://doi.org/10.1016/j.matlet.2017.06.053.
66. Thomas, M. E., Tropf, W. J., *Handbook of Optical Constants of Solids*, Elsevier Science, 1998.
67. Irfan, M., Shakoor, A., "Structural, Electrical and Dielectric Properties of Dodecylbenzene Sulphonic Acid Doped Polypyrrole/Nano-Y_2O_3 Composites", *J. Inorg. Organomet. Polym. Mater.*, 30 (2020) 1287–1292. https://doi.org/10.1007/s10904-019-01287-w.
68. Yan, Y., Yang, G., Xu, J. -L., Zhang, M., Kuo, C. -C., Wang, S. -D., "Conducting polymer-inorganic nanocomposite-based gas sensors: a review", *Sci. Technol. Adv. Mater.*, 21 (2020) 768–786. https://doi.org/10.1080/14686996.2020.1820845.
69. Bajantri, S. N., Mathad, R. D., "Effect of Energy Band Gap and Substrate Temperature on Gas Sensing Properties of F and PEG-6000 Co-Doped SnO_2 Thin Films", *International Journal of Pure and Applied Physics*, 13 (2017), 219-229.
70. Sekhar, M. C., Ramana, M. V., "Instant Synthesis of ZnO Nanoparticles by Microwave hydrothermal Method", *Int. J. Nanosci. Nanotechnol.*, 8 (2017) 174-23.
71. Fatima, A. A., Devadason, S., "Influence of Multilayers on Structural, Morphological, Luminescence and Magnetic Properties of ZnO Think Films", *Int. J. Nanosci. Nanotechnol.*, 3 (2011) 249-258.